

TECHNISCHE UNIVERSITÄT BERLIN  
Fakultät IV - Elektrotechnik und Informatik  
Institut für Technische Informatik und Mikroelektronik  
Dept. Computational Psychology

Abschlussarbeit

---

Comparing the Performance of Computational Models of  
Human Visual Perception Through Parametric Variations  
in Visual Stimuli

---

vorgelegt von  
**CLARA OLLECH**  
zur Erlangung des akademischen Grades  
Bachelor of Science (B.Sc.)  
im Studiengang Informatik

**Erstgutachterin:** Prof. Dr. MARIANNE MAERTENS  
**Zweitgutachter:** Prof. Dr. GUILLERMO GALLEG

19. August 2024



## SELBSTÄNDIGKEITSERKLÄRUNG

---

Hiermit erkläre ich, dass ich die vorliegende Arbeit selbstständig und eigenhändig sowie ohne unerlaubte fremde Hilfe und ausschließlich unter Verwendung der aufgeführten Quellen und Hilfsmittel angefertigt habe.

Berlin, den 19. August 2024



Clara Ollech



## ABSTRACT

---

Computational models for human brightness perception simulate specific mechanisms that likely contribute to perceiving various brightness effects. One particularly successful approach is the spatial filtering model known as the ODOG model, which has further developments, LODOG and FLODOG. LODOG incorporates local normalization, while FLODOG adds both local and frequency-specific normalization to enhance biological plausibility. To compare these models and get more detailed insight into the factors influencing their performance, they were applied to stimuli including White's effect, checkerboard, and bullseye illusions, with variations in spatial frequency and target size. Results show that ODOG and LODOG perform similarly, predicting the same effects with different magnitudes. FLODOG is more likely to predict assimilation and shows a stronger magnitude of effect for bullseyes and checkerboards. All models predict stronger assimilation at higher spatial frequencies and more contrast at larger target sizes, with FLODOG being less consistent to changes in target size than the other two. These findings highlight model behaviors, but psychophysical data is needed to determine which model most accurately reflects human brightness perception.

## ZUSAMMENFASSUNG

---

Rechenmodelle zur menschlichen Helligkeitswahrnehmung simulieren spezifische Mechanismen, die wahrscheinlich zur Wahrnehmung verschiedener Helligkeitseffekte beitragen. Ein besonders erfolgreicher Ansatz ist das räumliche Filtermodell ODOG, das weiterentwickelt wurde zu LODOG und FLODOG. LODOG beinhaltet lokale Normalisierung, während FLODOG sowohl lokale als auch frequenzspezifische Normalisierung hinzufügt, um die biologische Plausibilität zu erhöhen. Um diese Modelle zu vergleichen und detailliertere Einblicke in die Faktoren zu erhalten, die ihre Leistung beeinflussen, wurden sie auf Reize wie den White's Effekt, Checkerboard- und Bullseye-Illusionen angewendet, wobei diese in der räumlichen Frequenz und der Test Patch Größe variiert wurden. Die Ergebnisse zeigen, dass ODOG und LODOG ähnlich funktionieren und dieselben Effekte mit unterschiedlichen Intensitäten vorhersagen. FLODOG neigt dazu, Assimilation vorherzusagen und zeigt eine stärkere Wirkung bei Bullseye- und Checkerboard-Illusionen. Alle Modelle sagen eine stärkere Assimilation bei höheren räumlichen Frequenzen und mehr Kontrast bei größeren Test Patches voraus, wobei FLODOG weniger konsistent auf Änderungen der Test Patches reagiert als die anderen beiden Mo-

delle. Diese Erkenntnisse heben die Verhaltensweisen der Modelle hervor, aber es sind psychophysische Daten erforderlich, um zu bestimmen, welches Modell die menschliche Helligkeitswahrnehmung am genauesten widerspiegelt.

## ACKNOWLEDGMENTS

---

I want to thank Dr. Joris Vincent for his help in choosing my thesis topic and for his support throughout the process. His constructive feedback was a big help in guiding me as I worked on my thesis.



## CONTENTS

---

1	Introduction	1
1.1	Luminance and Brightness . . . . .	1
1.2	Models for Brightness Perception . . . . .	3
1.3	ODOG, LODOG and FLODOG . . . . .	4
2	Method	9
2.1	Models, Stimuli and Parameters . . . . .	9
2.2	Model Comparison . . . . .	12
3	Results	15
3.1	White's illusions . . . . .	15
3.2	Checkerboard Illusions . . . . .	16
3.3	Bullseye Illusions . . . . .	17
4	Discussion	21
	References	25

## LIST OF FIGURES

---

Figure 1.1	Visualisation of illumination, reflectance and luminance . . . . .	1
Figure 1.2	Picture of a scene showing the difference between lightness and brightness . . . . .	2
Figure 1.3	Simultaneous contrast and White's effect . . . . .	3
Figure 1.4	Functionality of the ODOG model . . . . .	5
Figure 2.1	White's illusions varying in spatial frequency and target height . . . . .	10
Figure 2.2	Checkerboard illusions varying in spatial frequency . . . . .	11
Figure 2.3	Bullseye illusions varying in spatial frequency . . . . .	12
Figure 2.4	Bullseye illusions varying in spatial frequency and target size . . . . .	13
Figure 3.1	Results for White's illusions . . . . .	16
Figure 3.2	Results for checkerboard illusions . . . . .	17
Figure 3.3	Results for first set of bullseye illusions . . . . .	18
Figure 3.4	Results for second set of bullseye illusions . . . . .	20

## INTRODUCTION

---

### 1.1 LUMINANCE AND BRIGHTNESS

When light hits an object, some of it reflects and reaches the human eye. The human visual system then processes this light to form a perception of the object. The term "illumination" describes the incoming light onto a surface, "reflectance" denotes the proportion of light that is subsequently reflected from the surface, and "luminance" characterizes the amount of light that ultimately reaches the eye([Adelson, 2000](#); [F. A. A. Kingdom, 2014](#); [Murray, 2021](#)). See Figure 1.1.

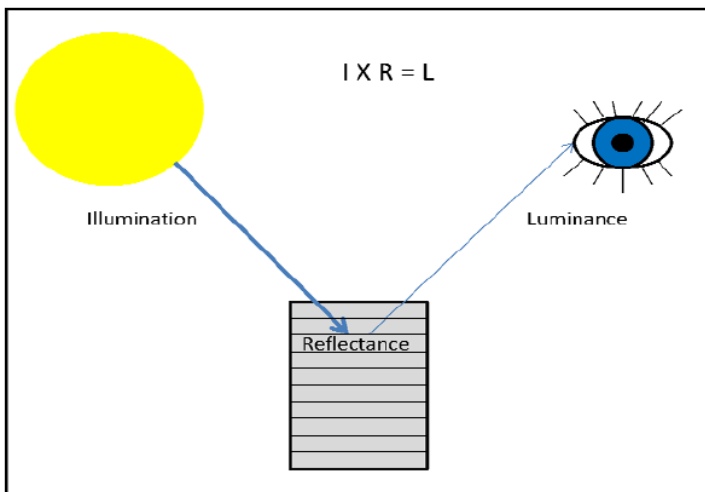


Figure 1.1: Visualisation of illumination, reflectance, and luminance. The blue arrow from the light source to the object represents illumination, which is the light falling on the object. The object reflects part of that light. Luminance, represented by the slender blue arrow in the image, is the reflected light that reaches the observer's eye. Luminance is therefore the product of Illumination and Reflectance. Image by [Riddle \(2011\)](#).

The human visual system attempts to determine the reflectance and illumination of an image using only the luminance captured by the eye, and it is generally quite effective at doing so. Hence, we can distinguish whether a surface in an achromatic image is painted in a darker color (reflectance) or is situated in shadow (illumination), even when the greyscale shades are identical. This perceptual ability is known as lightness constancy, with lightness itself being the perceived reflectance of an object. In contrast, brightness refers to the perceived luminance or, in simpler terms, the intensity of light as perceived ([Adelson, 2000](#); [F. A. Kingdom, 2011](#)). For example, in Figure 1.2, the

walls of the house appear to be uniformly painted white. This is a lightness judgement as the walls are reflecting a consistent proportion of the incident light. However, the walls are still brighter in some places than others. This is a brightness judgement as there shines more light on some parts of the walls while other parts lie in shadow.



Figure 1.2: A picture of a scene helps to show the difference between lightness and brightness. The house walls appear to be painted the same light color (a lightness judgment), but they look brighter in some places and darker in others because of shadows and shading (a brightness judgment). Image by [F. A. Kingdom \(2011\)](#).

Brightness or lightness illusions are scenes without visible illumination (Figure 1.3). For such scenes the terms brightness and lightness become synonymous ([Blakeslee, Reetz, and McCourt, 2008](#); [F. A. A. Kingdom, 2014](#)). Brightness illusions are intriguing because the visual system perceives them differently than their physical description. For example in a contrast effect two squares with the same shade of grey, situated on different backgrounds are often perceived differently (see Figure 1.3). The square on the darker background is perceived as lighter or brighter than the square on the darker background. Contrast therefore entails a shift in the brightness of the test patch away from the region it borders. Other illusions work in the opposite direction meaning that an area is perceived lighter than it actually is when mainly surrounded by a lighter region and darker when surrounded by a darker region. This effect that involves a shift in the brightness of the test patch towards the regions with which it shares a greater border with is called assimilation ([F. A. Kingdom, 2011](#); [F. A. A. Kingdom, 2014](#)). In conclusion the brightness perception of an area is strongly dependent on the surrounding context. Consequently, optical illusions provide valuable insights into understanding the workings of the visual system and the factors that influence it ([Adelson, 2000](#)).

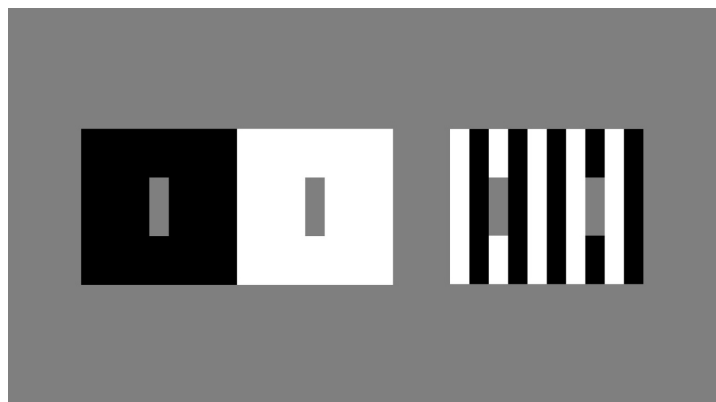


Figure 1.3: The left stimuli shows a brightness contrast effect. Despite sharing identical luminance values, the left rectangle against the black background appears lighter compared to the right rectangle. The right stimulus is a White's illusion and shows an assimilation effect. While both grey rectangles have the same luminance, the ones flanked by black appear darker than the rectangles flanked by white. Image created with stimupy by [Schmittwilken et al. \(2023\)](#).

## 1.2 MODELS FOR BRIGHTNESS PERCEPTION

While it is clear that the surrounding context significantly influences the perception of brightness on a surface, the exact mechanisms by which this occurs are complex. Different theories suggest that this influence involves a range of processes, low-level vision involves the earliest stages of visual processing, where the visual system begins to interpret raw sensory data from the eyes, focusing on basic tasks like edge and contrast detection. As processing continues, mid-level vision organizes these features through contour integration and grouping. Finally, high-level cognitive processes use interpretation and prior knowledge to understand the scene. Most likely, all three levels combine to enable the perception of brightness ([Adelson, 2000](#); [Robinson, Hammon, and de Sa, 2007](#)).

Numerous models attempt to replicate the mechanisms of brightness perception, ranging from low-level to high-level processes ([F. A. Kingdom, 2011](#); [F. A. A. Kingdom, 2014](#)). Modeling these approaches is important; if a model accurately predicts brightness perception, it suggests that the mechanisms it represents are likely significant components of the human visual system. Conversely, if a model is unsuccessful, it indicates that the mechanisms it represents might be less important or incorrectly modeled.

A quite successful approach are spatial filtering models as they are able to account for numerous brightness illusions ([F. A. Kingdom, 2011](#); [Murray, 2021](#)). Spatial filtering models are a low-level approach imitating the functionality of cells located at the retina that will be further explained in section [1.3](#).

These spatial filtering models receive an achromatic image as input and by applying spatial filters generate an output image that predicts the human perception of brightness for that specific input. Depending on the filters applied to the image certain calculations depending on the greyscale value of the pixel and its neighbors is performed, generating a new greyscale value for each pixel (Gonzalez and Woods, 2017).

There are a variety of spatial filtering models (Dakin and Bex, 2003; F. A. Kingdom, 2011). Among them, I will focus on the ODOG model by Blakeslee McCourt (Blakeslee and McCourt, 1999), as it is often regarded as the most successful of its kind (Economou, Zdravkovic, and Gilchrist, 2007; Kim, Gold, and Murray, 2018). Additionally, I will also examine its further developments, the LODOG and FLODOG models. The models can be applied to any image, making them convenient for testing on brightness illusions, that were discussed earlier (section 1.1).

### 1.3 ODOG, LODOG AND FLODOG

All three models, ODOG, LODOG, and FLODOG, are based on the principles of difference-of-Gaussian (DoG) filters. These filters differ in scales, with "larger filters" being better suited for detecting broader, low-frequency patterns, and "smaller filters" more effective at detecting fine, high-frequency patterns. Blakeslee and McCourt (1997) discovered that the output from an array of seven DoG filters could effectively account for brightness illusions such as grating induction and simultaneous brightness contrast (Blakeslee and McCourt, 1997; Moulden and Kingdom, 1989). The DoG filters mimic the functionality of the center-surround inhibition of ganglion cells located at the retina. The receptive fields of ganglion cells consist of an inner and an outer circle. Activation occurs when light stimulates the inner region, while inhibition is triggered when light affects the outer region (Kuffler, 1953; Murray, 2021). DoG filters model this receptive field with a positively weighted center Gaussian and a negatively weighted surround Gaussian. The size of the center and surround varies depending on the scale of the filter, allowing different filters to detect features of varying spatial frequencies.

The Oriented Difference of Gaussians (ODOG) model by Blakeslee and McCourt (1999) extends the basic principles of the DoG filter to better account for the orientation selectivity observed in human visual perception. While traditional DoG filters are isotropic and respond equally to all orientations, the ODOG model incorporates orientation specificity by using multiple DoG filters, each tuned to different orientations. The filters are therefore not circular but elliptic with each filter featuring a positive, circularly symmetric center and a negative, elongated surround (Robinson et al., 2007). The ODOG

model also adds response normalization, a process that helps maintain consistent perception of sensory information, such as sight and sound, by adjusting sensitivity to changes in the environment (Geisler and Albrecht, 1995).

The ODOG model applies those 7 DoG filters at 6 different orientations to an image. The outputs from these 42 oriented filters are combined across frequency and normalized within orientation using a global measure based on the overall energy across the entire image for each pixel. The normalized responses from all orientations are combined to form the final output providing a detailed, point-by-point prediction of the input image's perceived brightness (Robinson et al., 2007). Figure 1.4 provides a detailed overview of the steps involved in the ODOG model.

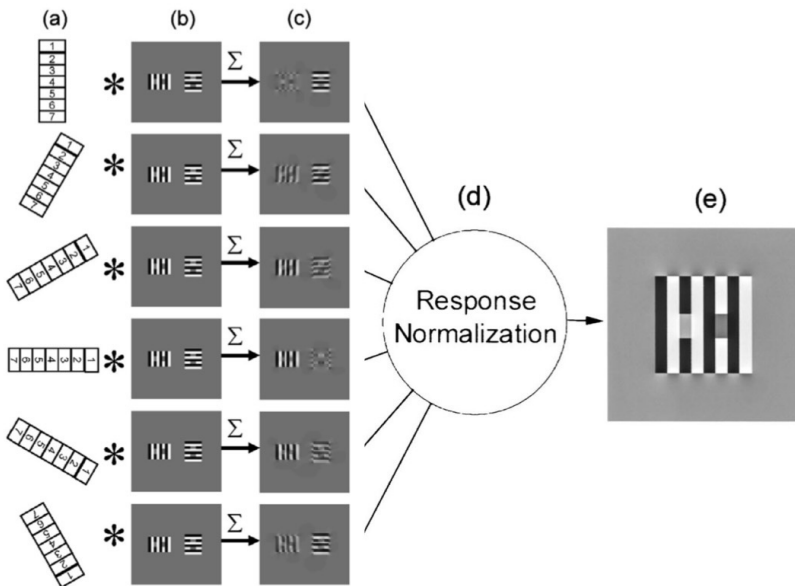


Figure 1.4: Representation of the functionality of the ODOG model. (a) Representation of the 42 filters, varying across 7 scales and 6 orientations. (b) The input image. (c) The outcome of applying a to b and summing across frequencies. (d) The six summed responses are normalized globally within each orientation and combined afterwards. (e) The final model output. Image combined from Blakeslee et al. (2008) and Robinson et al. (2007).

While the ODOG model is used quite commonly and often referred to as a successful model for a low-level approach in brightness perception Robinson et al. (2007) extended the ODOG model by adding components to the normalization step of the model. Consequently they

introduced the locally-normalized ODOG model (LODOG). LODOG, integrates local normalization by emphasizing the concept that areas in close proximity to the test patch exert a more substantial influence on its brightness perception than arbitrary regions across the stimulus, making it more neurally plausible. LODOG applies the same 42 filters to the input image as ODOG and also sums the responses across different frequencies. However the following normalization (Figure 1.4, d) for each pixel no longer depends on the energy across the entire scene. Instead the normalization value is calculated based on a Gaussian weighted window centered around the pixel. [Robinson et al. \(2007\)](#) tried Gaussian normalization windows with standard deviations of 1, 2 and 4 degrees of visual angle with the version with 4° proved to be the most successful.

Moreover, research indicates that neurons in the visual cortex with similar preferences for spatial frequencies tend to be in close proximity, suggesting that lateral inhibition by a neuron should impact neighboring neurons with similar spatial frequency preferences ([Issa, Trepel, and Stryker, 2000](#); [Tootell, Silverman, and De Valois, 1981](#)). Consequently the frequency-specific LODOG (FLODOG) was developed ([Robinson et al., 2007](#)).

FLODOG refines the approach introduced by LODOG by incorporating frequency-dependent normalization windows. While it still applies the same set of 42 filters as ODOG and LODOG, FLODOG assigns varying weights to each filter based on their frequency, adjusting their contributions according to the relative frequency responses of nearby filters within the local spatial context of the image. These weighted responses are then used to calculate the normalization value. FLODOG therefore considers nearby pixels and other filter responses within the same orientation but at other frequencies for each pixel's normalization.

Robinson and colleagues evaluated the ODOG model and their extensions using 28 different stimuli, including variations of White's effect, radial White's effect, bullseye illusions, simultaneous brightness contrast, the Todorovic illusion, checkerboards, and the Benary cross. They found that ODOG and LODOG generally predicted similar effects. However, the checkerboard, bullseye, and radial White's illusions were particularly noteworthy because FLODOG predicted different effects for these stimuli compared to ODOG and LODOG.

[Blakeslee and McCourt \(2004\)](#) compared the outputs of ODOG models with empirical measurements of human brightness perception. They tested White's illusion and checkerboards, varying spatial frequency for both and test patch height for White's illusion. Observers noted an assimilation effect for White's illusion, that strengthens at higher spatial frequencies. This was observed by other sources as well

(Anstis, 2005; Blakeslee and McCourt, 1999; Yund and Armington, 1975). However the magnitude of White's decreases with increasing test patch height. For the checkerboard illusion, high spatial frequencies caused an assimilation effect, while low frequencies caused a contrast effect. The ODOG model accurately predicted changes in White's effect with spatial frequency but failed with varying test patch height. It also accounted for the checkerboard illusion effects.

Nedimović, Zdravković, and Domjan (2022) tested several models, including ODOG, LODOG, and FLODOG, on their ability to simulate human brightness perception for White's illusion at a low spatial frequency, a rectangular bullseye, and a checkerboard illusion. They found that only FLODOG accurately predicted the effects for the bullseye and checkerboard illusions, as well as matching empirical data for White's illusion.

Bakshi, Roy, Mallick, and Ghosh (2016) and Mitra, Mazumdar, Ghosh, and Bhaumik (2018) compared the ODOG model's predictions with experimental observations for White's effect. They created various stimuli by altering the test patch height and spatial frequency. Their findings showed that ODOG transitions from predicting assimilation to predicting contrast at high test patch heights, regardless of the frequency.

In general, higher spatial frequencies lead to a stronger perceived assimilation effect by humans across stimuli, while lower spatial frequencies can result in a transition to a contrast effect. ODOG typically predicts assimilation for White's effect and correctly anticipates intensity changes with increasing frequency, but it predicts contrast for high test patches. LODOG and FLODOG have undergone less testing; however, LODOG appears similar to ODOG, while FLODOG successfully accounts for bullseye and checkerboard illusions. Sources provide contradictory results on ODOG's performance with checkerboards, and there are no results for LODOG and FLODOG with varying spatial frequency and test patch height.

By systematically varying those two parameters within the different stimuli, I can potentially identify the factors influencing the divergent performance of ODOG, LODOG and FLODOG more accurately. This exploration not only contributes to understanding the models and their differences, but also shows which stimuli, when tested on humans, can provide valuable insights into the functionality of human visual perception, as the models might vary strongly for certain stimuli or could show a switch between contrast and assimilation for certain parameters and so on.

Based on this, the performance of ODOG, LODOG, and FLODOG is evaluated on three illusions: White's effect, the bullseye illusion, and the checkerboard illusion. I will explore the model responses

for variations in spatial frequency and test patch height for both the bullseye illusion and White's effect, along with variations in spatial frequency for the checkerboard illusions. This approach aims to pinpoint and characterize the specific conditions or parameters that lead to divergent performances among these models.

# 2

## METHOD

---

To investigate how and where the ODOG, LODOG and FLODOG model differ specifically, each model is applied to sets of stimuli, including White's illusion, checkerboards and bullseye illusions. These stimuli will vary in either spatial frequency and test patch height or just spatial frequency. From each model response, a single value representing the direction of effect (assimilation or contrast) and the magnitude of effect is calculated. The models are compared based on these values.

### 2.1 MODELS, STIMULI AND PARAMETERS

The stimuli are created with "stimupy," a package developed by the Department of Computational Psychology at Technische Universität Berlin ([Schmittwilken et al., 2023](#)). The exact code can be found in the repository [Ollech \(2024\)](#).

The size of all stimuli is expressed in degrees of visual angle, as the perceived size of a stimulus depends not only on its physical dimensions (in cm, inches, or pixels) but also on the distance between the stimulus and the observer. A large stimulus can appear small if viewed from a distance, and a small stimulus can appear large if viewed up close. To account for this, I specify the size of stimuli in degrees of visual angle, providing a clear and consistent measure of the stimulus size as it appears to the observer, regardless of the physical size of the image and its distance from the observer ([Schmittwilken et al., 2023](#)).

Each stimulus is surrounded by a grey background, which pads it to a total size of  $32 \times 32$  degrees. The background and the target or test patches for each stimulus have an intensity value of 0.5, where 0 represents black and 1 represents white. In the illusions, the bars in White's illusion, the checks in the checkerboard illusion, and the rings in the bullseye have intensity values of either 0 (black) or 1 (white).

For White's illusion, which consists of a square-wave grating, two test patches are placed on the grating. One patch is positioned on a black bar flanked by white bars, while the other is on a white bar flanked by black bars. The three models will be tested on 24 variations of this illusion. The stimulus covers a  $12 \times 12$  degree area. The variations include four different spatial frequencies within the grating: 0.25, 0.5, 1, and 2 cycles per degree of visual angle. Additionally, six different target heights will be tested: 0.25, 0.5, 1, 2, 4, and 6 degrees of visual angle (see Figure ??).

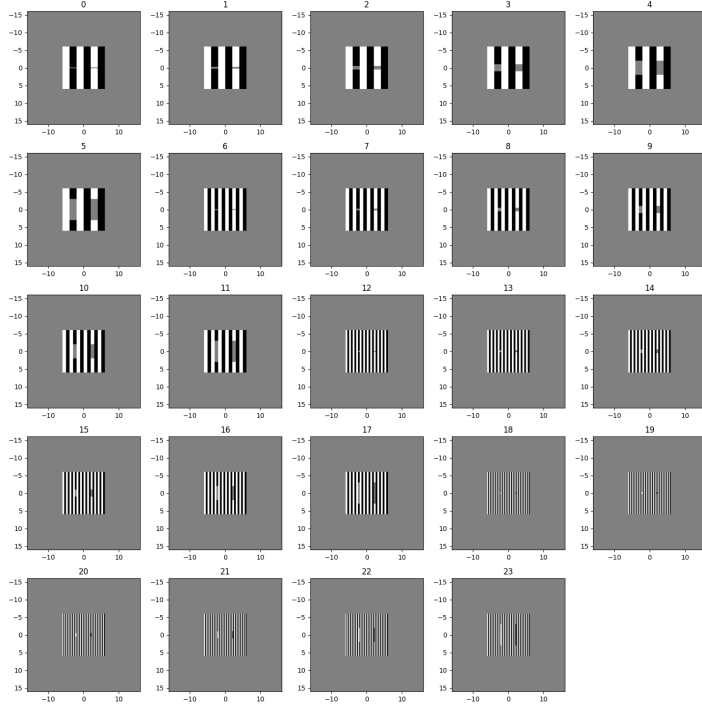


Figure 2.1: Variations of White’s effect. Each stimulus has a total size of  $32 \times 32$  degrees, including a grey background that is part of this overall size. The actual illusions are occupying a  $12 \times 12$  degree area. The background as well as the targets have a luminance of 0.5. The bars of the White’s illusion either have a luminance of 0 or 1 with 0 corresponding to the black bars and 1 to the white bars. The stimulus variations include four different spatial frequencies: 0.25, 0.5, 1, and 2 cpd of visual angle, as well as six different target heights: 0.25, 0.5, 1, 2, 4, and 6 degrees of visual angle.

Spatial frequency describes how often a pattern is repeated over a given distance and is expressed in cycles per degree (cpd) of visual angle, indicating the number of repetitions within one degree of visual angle. High spatial frequency refers to patterns with numerous fine details that change quickly over a short distance, such as thin stripes or small text. In contrast, low spatial frequency describes broad, smooth patterns with fewer changes over a longer distance. For example, in White’s illusion, a spatial frequency of 1 cpd means that within one degree of visual angle, there is one black bar and one white bar.

For the checkerboards, where two intersecting square-wave gratings form a checkerboard pattern, the targets are placed on individual checks. One target is positioned on a black check, predominantly surrounded by white checks, while the other is on a white check, mostly surrounded by black checks. The stimulus occupies a space of  $12 \times 12$  degrees and varies in spatial frequency. In this context, spatial frequency variation refers to changes in the number and size of the checks within the fixed stimulus size. A higher spatial frequency

corresponds to a greater number of smaller checks, while a lower spatial frequency results in fewer, larger checks. The stimuli vary in the following spatial frequencies: 0.25, 0.5, 0.75, 1, 1.25, 1.5, 1.75, and 2 cpd (see Figure 2.2).

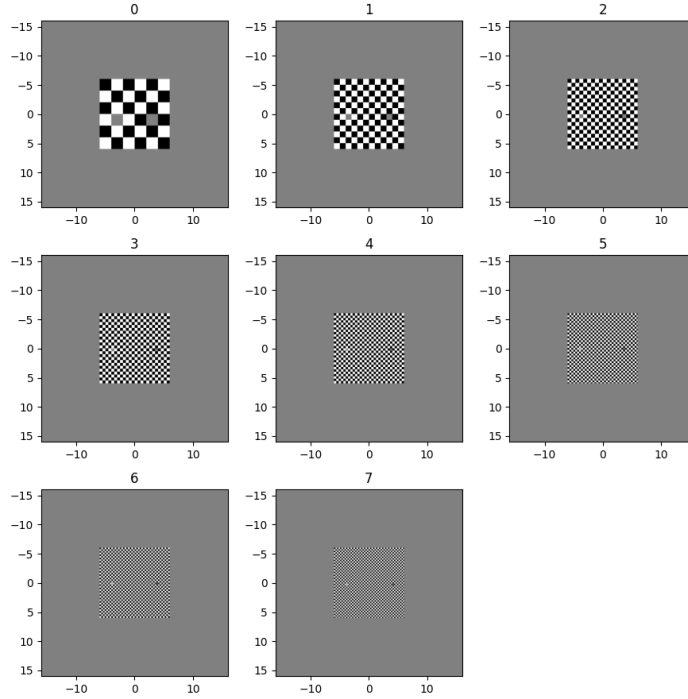


Figure 2.2: Variations of the checkerboard. Each stimulus has a total size of  $32 \times 32$  degrees, including a grey background that is part of this overall size. The actual illusions are occupying a  $12 \times 12$  degree area. The background as well as the targets have an intensity of 0.5. The checks either have an intensity of 0 or 1 with 0 corresponding to the black checks and 1 to the white checks. The variations include eight different spatial frequencies: 0.25, 0.5, 0.75, 1, 1.25, 1.5, 1.75, and 2 cpd of visual angle.

For the bullseye illusions the models are tested on two sets of stimuli. In both sets, the total visual size is  $32 \times 32$  degrees. Within this space, two bullseyes are placed, each with a radius of 8 degrees. A bullseye consists of a grey circular target disc surrounded by alternating black and white rings, forming a circular grating. The two bullseyes differ in that the black and white rings are inverted for one of them. This results in one bullseye having a white ring immediately surrounding the grey target, while the other has a black ring closest to the target. The first set of stimuli only varies in spatial frequency and therefore the number and thickness of rings. The following frequencies are explored: 0.2, 0.3, 0.4, 0.5, 0.6, 0.7, 0.8, 0.9, 1.0, 1.1, 1.2, 1.3, 1.4, 1.5, 1.6, 1.7, 1.8, 2.0, 2.2, 2.5, 3.0, 3.3, 4.0, 5.0 and 6.5 cpd (see Figure 2.3). The second set of stimuli varies in spatial frequency from 0.16 to 5

across 6 steps. Additionally, it varies in target size with the following values: 0.1, 0.5, 1, 2, 3, and 4 degrees (see Figure 2.4).

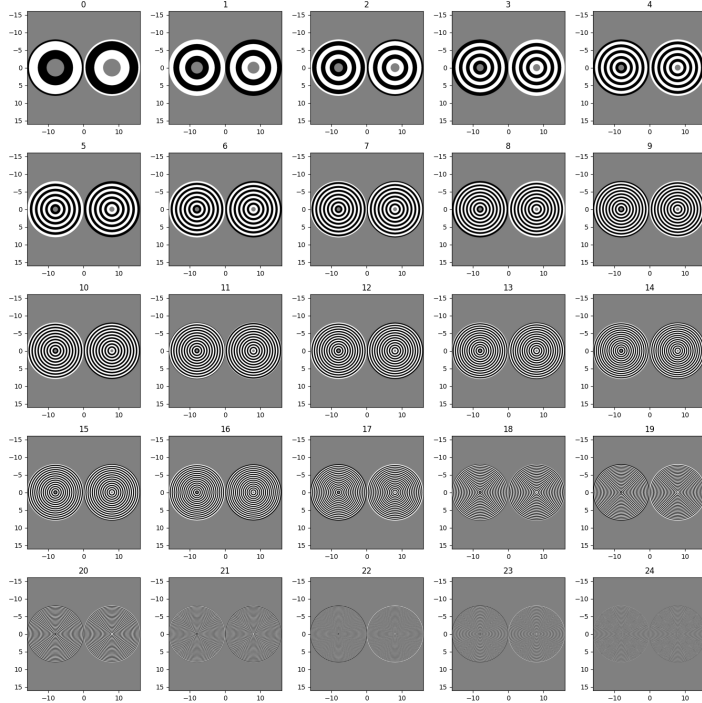


Figure 2.3: First set of variations of the bullseye illusion. Each stimulus has a total size of  $32 \times 32$  degrees. Each bullseye has a radius of 8 degrees. The background as well as the targets have an intensity of 0.5. The bars of the White's illusion either have an intensity of 0 or 1 with 0 corresponding to the black rings and 1 to the white rings. The variations include 25 different spatial frequencies: 0.2, 0.3, 0.4, 0.5, 0.6, 0.7, 0.8, 0.9, 1.0, 1.1, 1.2, 1.3, 1.4, 1.5, 1.6, 1.7, 1.8, 2.0, 2.2, 2.5, 3.0, 3.3, 4.0, 5.0 and 6.5 cpd of visual angle.

## 2.2 MODEL COMPARISON

The models are applied to every single stimulus using the "multyscale" package, also provided by the Department of Computational Psychology at Technische Universität Berlin ([Vincent, 2022](#)).

From the corresponding model output the predicted strength and direction, contrast or assimilation effect, of illusion will be calculated as a single value for every stimulus. For this purpose, each pixel in the model output is assigned a value based on its luminance ([Blakeslee and McCourt, 1999](#)). The higher the value, the higher the predicted brightness of that pixel. Subsequently, the average response for all pixels in each of the two test patches in each illusion is determined ([Robinson et al., 2007](#)). To obtain a single value that represents the predicted strength as well as the direction of an illusion by the model, the difference between the values for the two test patches is computed.

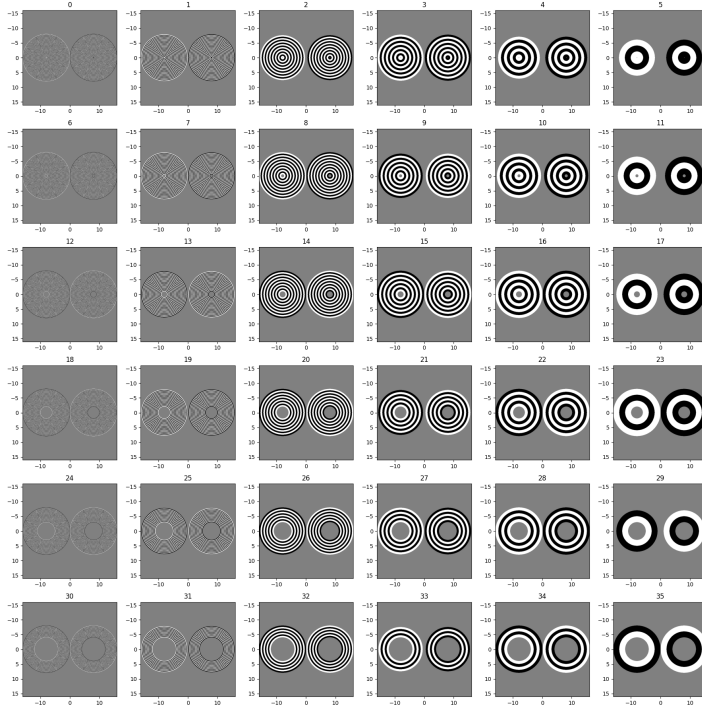


Figure 2.4: Second set of variations of the bullseye illusion. Each stimulus has a total size of  $32 \times 32$  degrees. Each bullseye has a radius of around 8 degrees. The background as well as the targets have an intensity of 0.5. The bars of the White's illusion either have an intensity of 0 or 1 with 0 corresponding to the black rings and 1 to the white rings. The variations include 6 different spatial frequencies spanning from approximately 0.2 to 5 cpd of visual angle. For the exact spatial frequency values see here([link to repository](#)). The stimuli also vary in 6 different target sizes: 0.1, 0.2, 0.5, 1.0, 3.0 and 4.0 degrees.

To ensure that the calculated value reflects the direction of effect, so either assimilation or contrast, the value for test patch that is mainly surrounded by black is subtracted from the test patch mainly surrounded by white. For example when the model predicts assimilation the test patch mainly surrounded by white will have a higher value than the test patch surrounded by black so a lower number is subtracted from a higher number creating a positive value. A positive value therefore stands for a predicted assimilation effect, a negative number for a contrast effect, and zero for no predicted effect at all, as both test patches have the same brightness according to the prediction of the model.

The White's illusion is unique because the surrounding amount of black and white varies with the test patch height, rather than the test patches being simply surrounded predominantly by black or white. For White's illusion, the effect is determined by subtracting the test patch flanked by black bars from the test patch flanked by white bars. For the White's illusion, I will use the terms assimilation and contrast

as follows: If the predicted test patch shows a shift in brightness towards the flanking bars, it is referred to as assimilation. If it shows a shift in brightness away from the flanking bars, it is referred to as contrast.

Since all three models differ in their normalization steps and thus perform different calculations, their predicted brightness intensities are not directly comparable. I will still analyze the magnitude of the effect for each model; however, to compare the magnitude of the effect between the models, a scaling method must be used to enable comparability.

Python 3.11.7 is used for the entirety of this thesis. Additionally, the Python packages Matplotlib, pandas, and seaborn were used for data exploring and processing as well as plotting the visualizations which are shown in Section 3.

# 3

## RESULTS

---

To get a deeper insight into how the ODOG, LODOG and FLODOG model perform, they are applied to four different sets of stimuli, including White's effect, checkerboards and the bullseye illusion. Within each set of stimuli either the spatial frequency or spatial frequency and target sized are varied. A single value representing the predicted direction and magnitude of the effect is calculated from the model output. This value is determined by the difference of predicted test patch brightness. A positive number stands for an assimilation effect, a negative number for a contrast effect. The further the value is from zero, the stronger the predicted effect of the illusion.

### 3.1 WHITE'S ILLUSIONS

For White's illusion ODOG and LODOG predict assimilation for almost all parametrizations as the calculated difference in patch brightness is positive in nearly all cases (Figure 3.1). The only exception occurs at the lowest frequency of 0.25 cycles per degree with the highest test patch height of 6 degrees, where the models predict contrast.

Additionally we can see an increase in the strength of predicted assimilation effect with increasing frequency for all target heights. The increase is most pronounced for the smallest target height (0.25), showing a steep and continuous rise. Larger target heights (1.0, 2.0, 4.0, 6.0) demonstrate a more moderate increase. At higher frequencies (2.0), the largest effect magnitude is observed, with the smallest target height (0.25) showing the maximum effect.

It is evident that smaller test patch heights result in a stronger predicted effect. For instance, even at the lowest frequency (0.25 cycles per degree), ODOG and LODOG predict a stronger assimilation effect for the smallest test patch height (0.25 degrees) than they do for a test patch height of 1 degree at the highest frequency of 2 cycles per degree. LODOG predicts the magnitude of effect for almost all illusions to be almost half as strong as those predicted by ODOG.

FLODOG also predicts assimilation for all illusions except the one with the lowest frequency and biggest target. In terms of sensitivity to frequency, the FLODOG model is more responsive to changes. This results in a more pronounced increase in effect as frequency increases.

FLODOG shows a more similar magnitude of effect to ODOG than LODOG, however while the ODOG model shows a similar peak for magnitude of effect, the overall magnitudes across all target heights are much lower for ODOG. It is also noticeable that, for the ODOG

and LODOG models, smaller target heights result in a significantly stronger predicted assimilation effect. This clear-cut pattern is not observed in the FLODOG model. Instead, the differences between the test patch heights are much smaller, with the strongest effect predicted for mid-range test patch heights, such as 0.5, 1, and 2 degrees of visual angle.

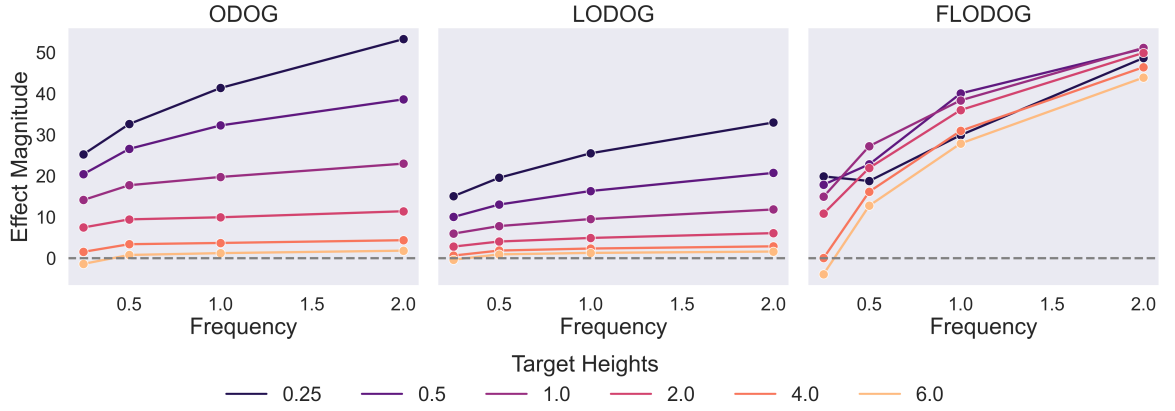


Figure 3.1: Results for variations of White’s Illusion. Each graph displays the outcomes for one of the models. The x-axis represents the spatial frequency of the stimulus, ranging from 0.25 to 2 cycles per degree (c/d). The colors indicate different target heights, which range from 0.25 to 6 degrees; darker colors correspond to smaller targets. The y-axis shows the effect magnitude and direction of effect. Positive values indicate an assimilation effect, while negative values indicate a contrast effect. The closer the values (and thus the lines) are to zero, the smaller the magnitude of the predicted effect.

### 3.2 CHECKERBOARD ILLUSIONS

For the checkerboards, FLODOG consistently predicts assimilation across all images (Figure 3.2). It is notable that higher frequencies result in a stronger predicted assimilation effect. For instance, for illusions with a frequency of 2 cycles per degree, the predicted effect is approximately six times stronger than for those with a frequency of 0.25 cycles per degree.

ODOG and LODOG both predict contrast for lower spatial frequencies ranging from 0.25 to 1.25 cycles per degree, and assimilation for high frequencies from 1.5 to 2 cycles per degree. The magnitude of the assimilation effect increases with higher frequencies.

ODOG predicts a stronger effect than LODOG in both the directions of contrast and assimilation, with the magnitude of the effect being about twice as strong in the ODOG model compared to the LODOG model. FLODOG predicts a much stronger magnitude of effect for all

illusions. While ODOG and LODOG range between -2 and 2, FLODOG ranges from 10 to 60.

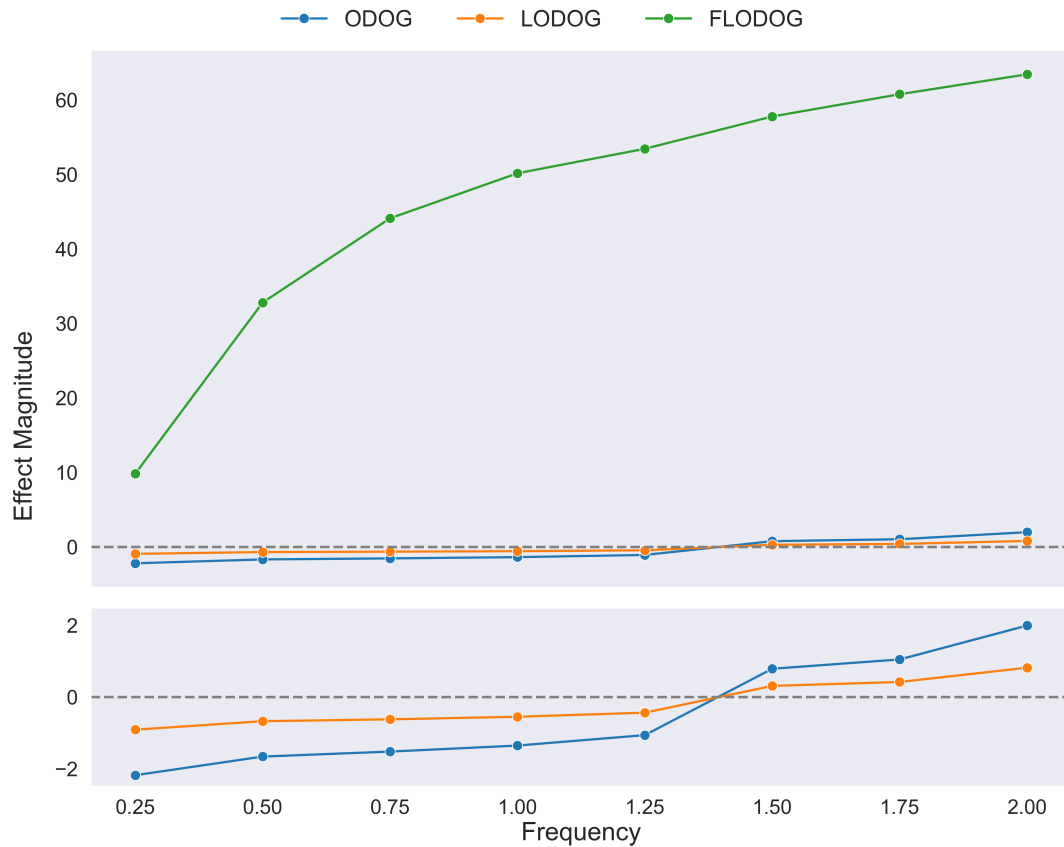


Figure 3.2: Results for the checkerboard illusions. In both graphs, the blue line represents the results for ODOG, the orange line represents the results for LODOG, and the green line represents the results for FLODOG. The x-axis represents the frequency, ranging from 0.25 to 2.0 cycles per degree, while the y-axis shows the effect magnitude and direction for each model. Positive values indicate an assimilation effect, and negative values indicate a contrast effect. The closer the values (and thus the lines) are to zero, the smaller the magnitude of the predicted effect. The second graph provides a close-up view of the first graph, with the y-axis limited to -2.5 to 2.5, making it easier to observe the behavior of ODOG and LODOG.

### 3.3 BULLSEYE ILLUSIONS

I tested the models on two sets of bullseye stimuli, one varying in spatial frequency, the other varying spatial frequency as well as target size.

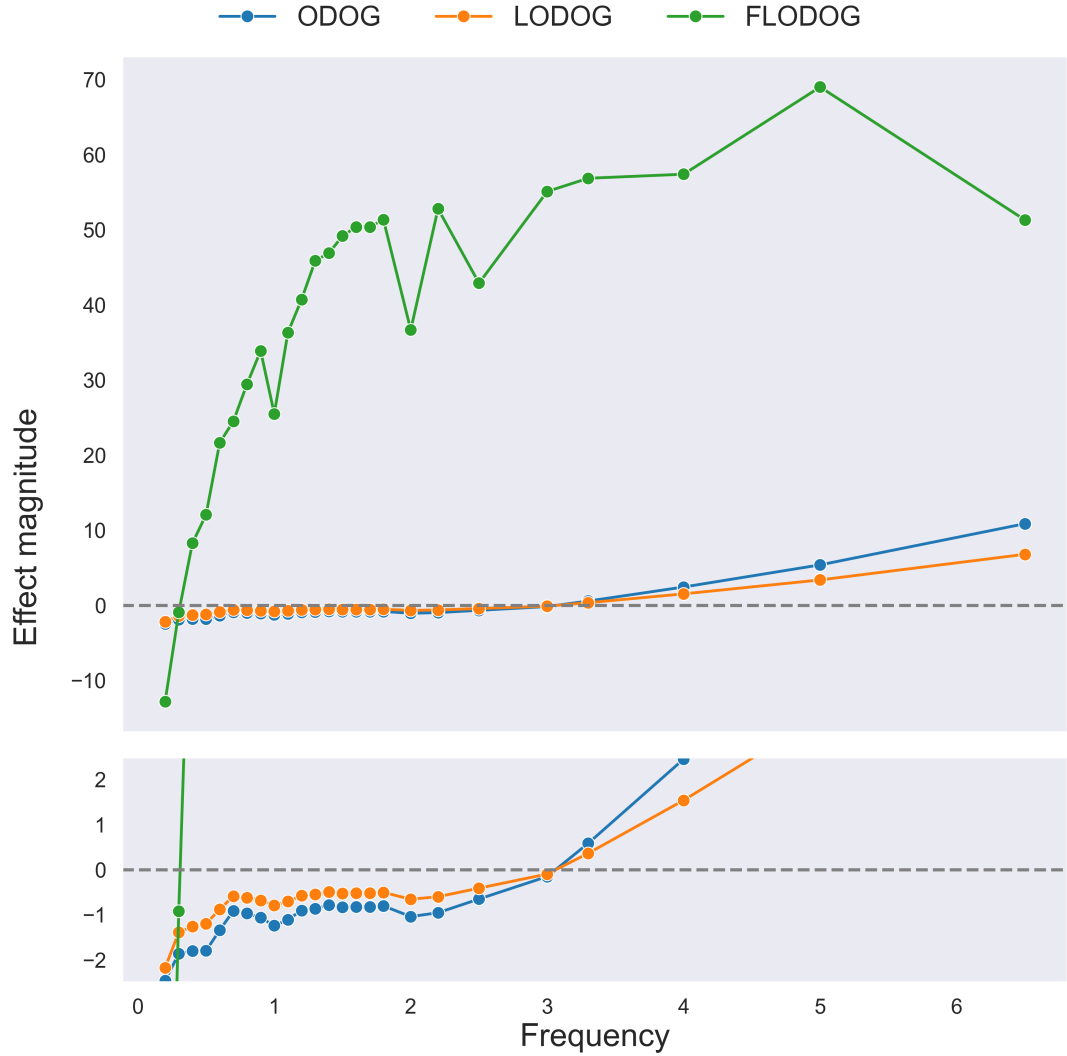


Figure 3.3: Results for the Bullseye Illusion varying only in spatial frequency.

The blue line represents the results for ODOG, the orange line represents the results for LODOG, and the green line represents the results for FLODOG. The x-axis indicates the spatial frequency of the checkerboard stimuli, while the y-axis shows effect magnitude and direction for each model. Positive values indicate an assimilation effect, and negative values indicate a contrast effect. The closer the values (and thus the lines) are to zero, the smaller the magnitude of the predicted effect. The second graph provides a close-up view of the first graph, with the y-axis limited to -2.5 to 2.5, making it easier to observe the behavior of ODOG and LODOG and see the crossover point from contrast to assimilation.

While only varying frequency, FLODOG predicts assimilation for all stimuli except those with the two lowest frequencies, 0.2 cycles per degree and 0.3 cycles per degree (Figure 3.3). Generally, the predicted effect increases with frequency, but the incline is not as smooth as it was for the checkerboard or White's illusions. The effect increases sharply up to around 2 cycles per degree, after which the increase

becomes uneven. For instance, the predicted effect at a frequency of 6.5 cycles per degree is weaker than at 5 cycles per degree.

ODOG and LODOG once again produce very similar predictions. Both models predict a contrast effect for frequencies up to 3 cycles per degree and assimilation for higher frequencies when the target size is fixed. For varying target sizes, ODOG and LODOG predict assimilation only for the smallest target size, but therefore for all frequencies except the lowest of 0.2 c/d. As observed in the checkerboard results, the lines representing the model results rise gradually for ODOG and LOODOG, indicating that the magnitude of the assimilation effect increases with frequency, while the magnitude of the predicted contrast effect decreases with increasing spatial frequency.

For the largest target size of 4 degrees, FLODOG predicts contrast at all frequencies. For the 3-degree target size, it predicts assimilation at mid-range frequencies and contrast at both the lowest and highest frequencies. For target sizes of 0.5, 1, and 2 degrees, FLODOG predicts contrast only at the lowest frequency, with assimilation at higher frequencies. Notably, the magnitude of the assimilation effect does not increase gradually with frequency for these target sizes but remains relatively consistent. For the smallest target size of 0.1 degrees, FLODOG predicts contrast up to a frequency of around 1 cycle per degree, beyond which it predicts assimilation with the effect's magnitude increasing significantly with frequency.

Lastly, FLODOG predicts a much stronger effect than both ODOG and LODOG, sometimes up to 20 times greater. Consistent with the results for the checkerboard and White's illusion, ODOG predicts a stronger effect in both directions (contrast and assimilation) compared to LODOG, approximately twice as strong.

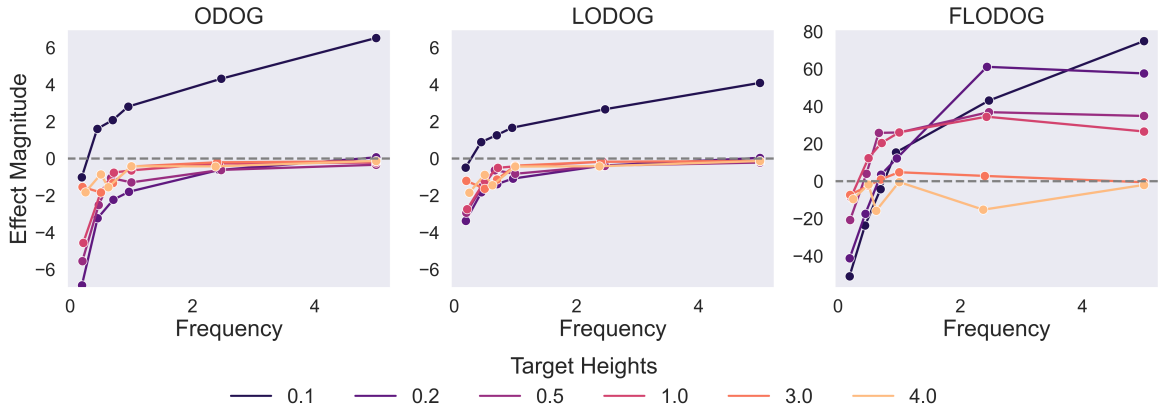


Figure 3.4: Results for variations of the bullseye illusion varying in spatial frequency and target size. Each graph illustrates the response of a different model (ODOG, LODOG, and FLODOG) to variations in the bullseye illusion. The x-axis represents the frequency, ranging from 0.2 to 5 cycles per degree, while the y-axis shows effect magnitude and direction for each model. Positive values indicate an assimilation effect, while negative values indicate a contrast effect. The closer the values (and thus the lines) are to zero, the smaller the magnitude of the predicted effect.

In summary, ODOG and LODOG show similar performance across all stimuli and parameters, with ODOG consistently predicting effects roughly twice as strong as those predicted by LODOG in both directions. FLODOG, on the other hand, predicts a similar effect magnitude for White's illusion but significantly stronger effects, around 10 to 20 times greater than those of ODOG or LODOG, for other illusions, demonstrating high sensitivity to changes in spatial frequency. For the bullseye and checkerboard illusions, FLODOG primarily predicts assimilation, while ODOG and LODOG predict contrast up to a high frequency before switching to assimilation. Additionally, all three models are more likely to predict assimilation or a stronger assimilation effect at higher frequencies. For ODOG and LODOG, smaller targets tend to result in predictions of assimilation and stronger assimilation effects. In contrast, FLODOG responds less consistently to changes in target size; however, very large targets lead to predictions of a contrast effect.

# 4

## DISCUSSION

---

There are various computational models designed to simulate the brightness perception of the human visual system based on specific approaches. One widely used and notably successful model is the ODOG model, a spatial filtering model developed by [Blakeslee and McCourt \(1999\)](#). Building on this, [Robinson et al. \(2007\)](#) developed two models, LODOG and FLODOG, aimed at improving the ODOG model. These models primarily differ in their normalization steps: LODOG introduces local normalization, while FLODOG incorporates both local and frequency-dependent normalization. These enhancements make the models more biologically plausible but also increase their complexity.

While the ODOG model has been extensively used and tested, there is less data on the performance of the LODOG and FLODOG models, raising questions about the stimuli and parameters that cause differences among the models. To compare these models, I tested them across a variety of stimulus sets, varying in both stimulus type and the parameters spatial frequency and target size, resulting in the following.

ODOG and LODOG showed a similar performance across all stimuli and parameters that I tested, which aligns with the findings of [Robinson et al. \(2007\)](#), who also reported that ODOG and LODOG generally predicted similar effects for the White's illusion, checkerboard and bullseye illusion.

[Robinson et al. \(2007\)](#) and [Nedimović et al. \(2022\)](#) additionally reported that FLODOG predicts a different effect for the checkerboard and bullseye illusions than ODOG and LODOG. My results confirm that observation for low and mid spatial frequency (see Figure 3.2 and 3.3). For high frequencies ODOG and LODOG switch from predicting a contrast effect to predicting a assimilation effect, matching FLODOG in the direction of predicted effect. [Robinson et al. \(2007\)](#) claim that the FLODOG is not able to account for the checkerboard illusion as it predicts assimilation at all spatial frequencies, while human observers tend to see a contrast effect at low frequencies and switch to assimilation at high frequencies, with the actual crossover point varying between subjects. As shown in Figure 3.2 ODOG and LODOG predict that crossover between 1.25 and 1.5 cpd, however it is unclear whether that crossover point matches the one observed by subjects.

Furthermore, the observation that all three models are more likely to predict assimilation or a stronger assimilation effect at higher fre-

quencies is consistent with the empirical observations of Blakeslee and McCourt (1999) who reported that observers are more likely to see an assimilation effect for high spatial frequencies in White's illusion, Yund and Armington (1975) and Anstis (2005) observed this as well. ODOG was able to account for that in the experiments of Blakeslee and McCourt (1999). My results build upon these observations by demonstrating that both LODOG and FLODOG also predict this effect. Furthermore, my findings reveal that this effect is not limited to White's illusion but extends to bullseye and checkerboard illusions for all three models.

An explanation for this pattern is that all three models predict stronger assimilation at high spatial frequencies because their filter responses as well as normalization processes inherently smooth out the rapid changes and dense details present in high-frequency patterns. This smoothing effect reduces the contrasts between closely spaced elements, leading to a more uniform and assimilated appearance (Blakeslee and McCourt, 2004).

Additionally, the impact of target size on the models is confirmed as well. Smaller targets result in stronger assimilation effects for these models, which aligns with the findings of Bakshi et al. (2016) and Mitra et al. (2018), who observed that ODOG transitions from predicting assimilation to predicting contrast at high test patch heights. This study further validates that smaller targets enhance the likelihood and magnitude of predicted assimilation effects for not only ODOG but LODOG as well. FLODOG in general predicts the same, showing a switch from assimilation to contrast at big targets in the bullseye and White's illusion.

That can be explained by the fact that large targets inherently contain more low-frequency information because the details are spread over a larger area. The visual models, which are effective at detecting these low-frequency details, enhance the contrast at the edges of the target. The models emphasize the differences between the target and the surrounding area, resulting in a stronger contrast effect. Smaller targets, similar to high frequency patterns are more likely to be smoothed out by the filters, reducing the contrast which leads to a more assimilated appearance.

However, while ODOG and LODOG consistently predict a stronger assimilation effect as the target size decreases, FLODOG is less consistent in this pattern. This inconsistency is a new finding that hasn't been reported before. It is evident in both the White's illusion (Figure 3.1) and the bullseye illusion (Figure 3.4).

Lastly my results really point out a difference in predicted magnitude of effect between the three models. My results consistently show that ODOG predicts an effect that is around twice as strong as

the effect predicted by LODOG. FLODOG, on the other hand, predicts a similar magnitude of effect for White's illusion but a much stronger effect (around 10-20 times as strong) for other illusion types like checkerboards and bullseyes.

The reason for the constant difference in effect magnitude between ODOG and LODOG lies in the normalization step. ODOG computes a normalization value for each pixel based on the energy of the entire stimulus, including the filter responses for the grey padding around the actual illusion. Since the filters in the models are designed to respond to differences, these uniform grey areas produce values close to zero in the filter response. As a result, the overall normalization value is significantly lower. This results in higher final response values in ODOG when each pixel is divided by this smaller normalization factor. In contrast, LODOG uses local normalization, which calculates a normalization value based on a smaller, localized area, leading to higher normalization values and consequently lower end response values.

FLODOG's strong response in magnitude of effect to changing spatial frequency makes sense as it is a lot more frequency sensitive, but it is unclear why FLODOG predicts such a strong effect for checkerboards and bullseye, or in other words why ODOG and LODOG predict such a small magnitude of effect for those specific illusions. While FLODOG consistently predicts similar magnitudes for all types of illusions, ODOG and LODOG show notably weaker effects for checkerboards and bullseyes compared to White's illusion. This discrepancy suggests that ODOG and LODOG struggle with accurately predicting the magnitude of these specific illusions. To properly analyze and interpret these differences in effect magnitude, psychophysical data and an effective scaling method are necessary.

It is particularly interesting that FLODOG is quite similar in magnitude of effect to ODOG and LODOG for White's illusion as [Robinson et al. \(2007\)](#) use a version of White's illusion to scale the model outputs to make them comparable. Such scaling is necessary because each model has different normalization steps and calculations, making their predicted brightness intensities not directly comparable. The results suggest that this kind of scaling worked out for White's illusion but might not be transferable to the other types of illusions. Standardizing the model outputs by setting the strength of the illusion for the stimulus to 1 reduces the predicted effect values. However, the substantial differences in the magnitude of effects for other illusions, apart from White's illusion, would remain. This is because the models predict a similar magnitude of effect for White's illusion. A different kind of scaling might be needed for each type of stimuli, or a in general more complex way of scaling might be useful.

These patterns of results can also be used to guide data collection with human observers. By comparing the patterns observed in the models' predictions with psychophysical data from human observers, the models' assumptions can be validated. This approach not only strengthens the credibility of the models but also deepens our understanding of how visual information is processed, potentially offering insights into the neural mechanisms involved in brightness perception. The role of local, global and frequency-specific normalization in these models may reflect similar processes in the human visual cortex.

Specifically, it would be interesting to determine whether humans exhibit the same consistency in predicting a stronger assimilation effect with smaller targets in White's illusion, which would align with the results from ODOG and LODOG.

On top of that, investigating whether humans show the switch from contrast to assimilation at higher frequencies in the checkerboard illusion, matching the predictions of ODOG and LODOG is also valuable.

Additionally if psychophysical data for the lower frequency versions of bullseye illusions aligns with FLODOG's predicted assimilation effect, it could underline the significance of frequency-specific normalization.

Finally, psychophysical data for all the stimuli tested here would be useful to compare the overall magnitude of effects between different types of stimuli. This could provide insight into the usefulness of the scaling method used by [Robinson et al. \(2007\)](#) and suggest ways to improve it if necessary.

## REFERENCES

---

- Adelson, E. H. (2000). 24 Lightness Perception and Lightness Illusions. Retrieved 2023-12-15, from <https://www.cs.unm.edu/~williams/cs591/Adelson.pdf>
- Anstis, S. (2005, November). White's Effect in Lightness, Color, and Motion. In M. R. M. Jenkin and L. R. Harris (Eds.), *Seeing Spatial Form* (p. o). Oxford University Press. Retrieved 2024-05-22, from <https://doi.org/10.1093/acprof:oso/9780195172881.003.0007> doi: [doi:10.1093/acprof:oso/9780195172881.003.0007](https://doi.org/10.1093/acprof:oso/9780195172881.003.0007)
- Bakshi, A., Roy, S., Mallick, A., and Ghosh, K. (2016, March). Limitations of the Oriented Difference of Gaussian Filter in Special Cases of Brightness Perception Illusions. *Perception*, 45(3), 328–336. Retrieved 2024-05-22, from <https://doi.org/10.1177/0301006615602621> (Publisher: SAGE Publications Ltd STM) doi: [doi:10.1177/0301006615602621](https://doi.org/10.1177/0301006615602621)
- Blakeslee, B., and McCourt, M. E. (1997). Similar mechanisms underlie simultaneous brightness contrast and grating induction. *Vision research*, 37(20), 2849–2869. Retrieved 2024-05-17, from <https://www.sciencedirect.com/science/article/pii/S0042698997000862> (Publisher: Elsevier)
- Blakeslee, B., and McCourt, M. E. (1999, December). A multiscale spatial filtering account of the White effect, simultaneous brightness contrast and grating induction. *Vision Research*, 39(26), 4361–4377. Retrieved 2024-01-09, from <https://www.sciencedirect.com/science/article/pii/S0042698999001194> doi: [doi:10.1016/S0042-6989\(99\)00119-4](https://doi.org/10.1016/S0042-6989(99)00119-4)
- Blakeslee, B., and McCourt, M. E. (2004). A unified theory of brightness contrast and assimilation incorporating oriented multiscale spatial filtering and contrast normalization. *Vision research*, 44(21), 2483–2503. Retrieved 2024-05-19, from <https://www.sciencedirect.com/science/article/pii/S0042698904002494> (Publisher: Elsevier)
- Blakeslee, B., Reetz, D., and McCourt, M. E. (2008). Coming to terms with lightness and brightness: Effects of stimulus configuration and instructions on brightness and lightness judgments. *Journal of Vision*, 8(11), 3–3. Retrieved 2024-05-21, from <https://iovs.arvojournals.org/article.aspx?articleid=2122090> (Publisher: The Association for Research in Vision and Ophthalmology)
- Dakin, S. C., and Bex, P. J. (2003, November). Natural image

- statistics mediate brightness 'filling in'. *Proceedings of the Royal Society B: Biological Sciences*, 270(1531), 2341–2348. Retrieved 2024-05-17, from <https://www.ncbi.nlm.nih.gov/pmc/articles/PMC1691518/> doi: doi:10.1098/rspb.2003.2528
- Economou, E., Zdravkovic, S., and Gilchrist, A. (2007). Anchoring versus spatial filtering accounts of simultaneous lightness contrast. *Journal of vision*, 7(12), 2–2. Retrieved 2024-05-22, from <https://iovs.arvojournals.org/article.aspx?articleid=2192940> (Publisher: The Association for Research in Vision and Ophthalmology)
- Geisler, W. S., and Albrecht, D. G. (1995). Bayesian analysis of identification performance in monkey visual cortex: nonlinear mechanisms and stimulus certainty. *Vision research*, 35(19), 2723–2730. Retrieved 2024-05-30, from <https://www.sciencedirect.com/science/article/pii/004269899500029Y> (Publisher: Elsevier)
- Gonzalez, R., and Woods, R. (2017). *Digital Image Processing*. Retrieved 2024-05-29, from <https://elibrary.pearson.de/book/99.150005/9781292223070> (ISBN: 9781292223070 Publisher: Pearson Deutschland)
- Issa, N. P., Trepel, C., and Stryker, M. P. (2000). Spatial frequency maps in cat visual cortex. *Journal of Neuroscience*, 20(22), 8504–8514. Retrieved 2024-05-19, from <https://www.jneurosci.org/content/20/22/8504.short> (Publisher: Soc Neuroscience)
- Kim, M., Gold, J. M., and Murray, R. F. (2018, December). What image features guide lightness perception? *Journal of Vision*, 18(13), 1. Retrieved 2024-05-17, from <https://doi.org/10.1167/18.13.1> doi: doi:10.1167/18.13.1
- Kingdom, F. A. (2011). Lightness, brightness and transparency: A quarter century of new ideas, captivating demonstrations and unrelenting controversy. *Vision Research*, 51(7), 652–673. Retrieved 2023-12-15, from <https://www.sciencedirect.com/science/article/pii/S0042698910004578> (Publisher: Elsevier)
- Kingdom, F. A. A. (2014). Brightness and Lightness. In J. S. Werner and L. M. Chalupa (Eds.), *The new visual neurosciences* (pp. 499–510). Cambridge, Massachusetts: The MIT Press.
- Kuffler, S. W. (1953, January). DISCHARGE PATTERNS AND FUNCTIONAL ORGANIZATION OF MAMMALIAN RETINA. *Journal of Neurophysiology*, 16(1), 37–68. Retrieved 2024-05-16, from <https://www.physiology.org/doi/10.1152/jn.1953.16.1.37> doi: doi:10.1152/jn.1953.16.1.37
- Mitra, S., Mazumdar, D., Ghosh, K., and Bhaumik, K. (2018, September). An adaptive scale Gaussian filter to explain White's illusion from the viewpoint of lightness assimilation for a large range of variation in spatial frequency of the grating and aspect ratio of the targets. *PeerJ*, 6, e5626. Retrieved 2024-05-22, from <https://>

- [peerj.com/articles/5626](https://peerj.com/articles/5626) doi: doi:10.7717/peerj.5626
- Moulden, B., and Kingdom, F. (1989, January). White's effect: A dual mechanism. *Vision Research*, 29(9), 1245–1259. Retrieved 2024-05-17, from <https://linkinghub.elsevier.com/retrieve/pii/0042698989900710> doi: doi:10.1016/0042-6989(89)90071-0
- Murray, R. F. (2021, September). Lightness Perception in Complex Scenes. *Annual Review of Vision Science*, 7(1), 417–436. Retrieved 2024-01-07, from <https://www.annualreviews.org/doi/10.1146/annurev-vision-093019-115159> doi: doi:10.1146/annurev-vision-093019-115159
- Nedimović, P., Zdravković, S., and Domijan, D. (2022, December). Empirical evaluation of computational models of lightness perception. *Scientific Reports*, 12(1), 22039. Retrieved 2024-05-17, from <https://www.nature.com/articles/s41598-022-22395-7> doi: doi:10.1038/s41598-022-22395-7
- Ollech, C. (2024). *Source code for bachelor thesis: Comparing performance of computational models of human visual perception*. Retrieved from <https://git.tu-berlin.de/claraollech/bachelorarbeit.git> (GitLab repository)
- Riddle, M. R. (2011). *The effects of stimuli type, size, and articulation on estimating the luminance contrast of real and crt targets*. Wake Forest University.
- Robinson, A. E., Hammon, P. S., and de Sa, V. R. (2007). Explaining brightness illusions using spatial filtering and local response normalization. *Vision research*, 47(12), 1631–1644. Retrieved 2023-12-15, from <https://www.sciencedirect.com/science/article/pii/S0042698907000648> (Publisher: Elsevier)
- Schmittwilken, L., Maertens, M., and Vincent, J. (2023). stimupy: A python package for creating stimuli in vision science. *Journal of Open Source Software*, 8(86), 5321. Retrieved from <https://doi.org/10.21105/joss.05321> doi: doi:10.21105/joss.05321
- Tootell, R. B., Silverman, M. S., and De Valois, R. L. (1981, November). Spatial Frequency Columns in Primary Visual Cortex. *Science*, 214(4522), 813–815. Retrieved 2024-05-19, from <https://www.science.org/doi/10.1126/science.7292014> doi: doi:10.1126/science.7292014
- Vincent, J. (2022, April). *Multyscale*. Berlin.
- Yund, E. W., and Armington, J. C. (1975, August). Color and brightness contrast effects as a function of spatial variables. *Vision Research*, 15(8), 917–929. Retrieved 2024-05-17, from <https://www.sciencedirect.com/science/article/pii/004269897590231X> doi: doi:10.1016/0042-6989(75)90231-X